Available online at www.sciencedirect.com
SCIENCE DIRECT®
Journal of Sound and Vibration 288 (2005) 1–32
JOURNAL OF SOUND AND VIBRATION
www.elsevier.com/locate/jsvi

Review

Aeroacoustics research in Europe: The CEAS-ASC report on 2004 highlights

J.A. Fitzpatrick

Department of Mechanical Engineering, Trinity College, Dublin University, Dublin 2, Ireland

Received 3 May 2005; accepted 5 May 2005
Available online 19 July 2005

Abstract

This paper summarizes some of the aeroacoustic research undertaken in Europe in 2004. It is compiled from information provided by the Aeroacoustics Specialists' Committee (ASC) of the Confederation of European Aerospace Societies (CEAS). The committee comprises representatives from the Aerospace Societies of France (AAAF), Germany (DGLR), Italy (AIDAA), The Netherlands (NVvL), Spain (AIAE), Sweden (SVFW) and the United Kingdom (RaeS) together with members from Greece, Ireland and Portugal.

Contents

E-mail address: john.fitzpatrick@tcd.ie.

0022-460X/$ - see front matter © 2005 Elsevier Ltd. All rights reserved.
doi:10.1016/j.jsv.2005.05.025

1. Introduction

The role of the Aeroacoustics Specialists' Committee of the CEAS is to promote and encourage aeroacoustics activities in the industrial and research communities in Europe. This paper gives a brief review of some of the activities conducted during 2004. Reports include aspects of a number of EU projects funded under the 5th and 6th Framework programmes including TurboNoiseCFD, JEAN, SILENCER, FACE and MESSIAEN. Enquiries concerning all contributions should be addressed to the authors who are given at the end of each subsection.

2. Fan and rotor noise

2.1. TurboNoiseCFD

In support of the 10 dB aircraft noise reduction objective of the Fifth Framework Programme, TurboNoiseCFD has created a new methodology that will improve the design of low noise turbomachinery components. This is based on the adaptation of *existing* computational fluid dynamics (CFD) software, significant developments of analytical and computational aeroacoustics (CAA) models for propagation and radiation and the development of a new, robust, matching

technique to couple CFD solutions with analytical or CAA models. A number of technical challenges have been successfully addressed and these include meshing, boundary conditions, dispersion, dissipation, nonlinear effects, excessive memory requirements and computational times.

The work comprised of four main workpackages, with the following objectives:

- *WP 1—noise requirements of CFD codes*—to identify the key features of CFD codes to model each type of turbomachinery tone noise source, including blade row transmission effects. To conduct a feasibility study into the CFD modelling of fan broadband noise sources.
- *WP 2—matching, propagation and radiation models*—to develop design rules for the matching of CFD solutions to current or refined propagation and radiation model(s) and produce source-to-far-field models.
- *WP 3—model testing and benchmarking*—to benchmark the methodology developed above against experimental data.
- *WP 4—low noise design improvement*—to apply the new methodology to low noise design concepts, to develop the tools in a working environment prior to exploitation and to recommend low noise concept improvements.

To demonstrate the methodology developed in WP 1 and WP 2, selected CFD/CAA codes have been successfully tested against experiment or analytic methods, as follows:

- Propagation in lined ducts versus RESOUND fan intake data; propagation through variable area intakes and bypass ducts versus a semi-analytic method.
- Fan rotor alone tones and buzz saw noise Versus in-duct FANPAC data; fan rotor alone tone radiation through a scarfed intake versus far-field RANNTAC data.
- Fan–OGV interaction tone noise generation versus in-duct RESOUND data.
- Fan–OGV interaction tone noise propagation through realistic engine type exhaust nozzle geometries and coaxial jet flows to the near and far-field, supported by comparisons with analytical solutions for simpler geometry/flow configurations.
- Rotor–stator interaction tones generated in three-stage turbine Versus RESOUND data.

In addition a feasibility assessment has been successfully completed on the CFD modelling of turbomachinery broadband noise sources.

[by A. Kempton, Rolls Royce, UK]

2.2. *A frequency domain method for rotor self-noise prediction*

A computer model for the prediction of broadband noise from an open rotor or propeller, as shown in Fig. 1, has been developed. It is assumed that the dominant source mechanism is by the interaction of the turbulent boundary with the rotor trailing edge. The model combines thin unsteady aerodynamic aerofoil theory with semi-empirical models for the boundary layer wavenumber frequency spectrum. The model has been used to undertaken parametric study in which the effect on broadband noise due to rotor chord, angle of attack numbers of blades, and rotor tip speed have been investigated. Validation of the model has been performed against the experimental data for a four-bladed Dowty Rotol R212 propeller (NACA 16 sections) of diameter

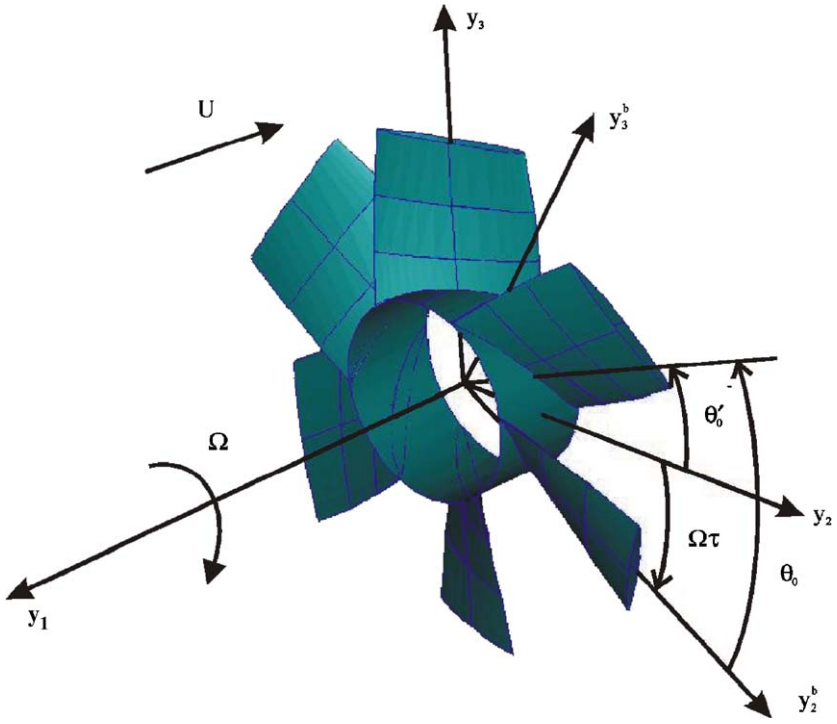

Fig. 1. Open rotor (or propeller) used in the broadband noise calculation.

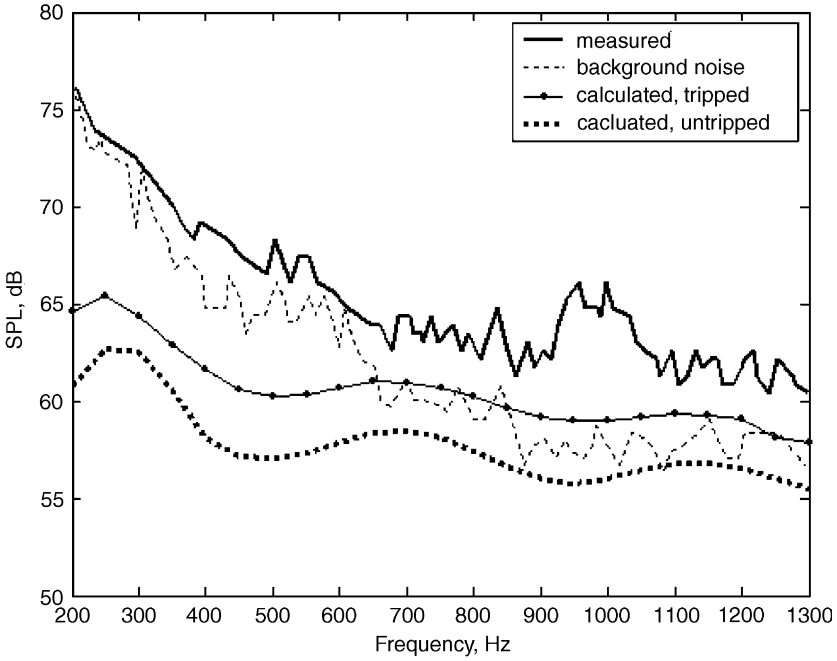

Fig. 2. Comparison between measured and predicted broadband noise for a four-bladed Dowty Rotol R212 propeller.

3.66 m. A comparison between the measured and predicted radiation spectrum in the transverse plane (i.e., 90° to the axis), 5.49 m from the axis, is plotted in Fig. 2. Spectral shape is reasonably well predicted with sound pressure levels predictions being observed to underestimate the measured spectrum by about 5 dB over the frequency range of interest.

[by Q. Zhou and P. Joseph, ISVR, University of Southampton, UK]

2.3. Hybrid CFD/acoustics for fluid machinery noise prediction

The practical application of numerical noise prediction methods such as CAA in the field of industrial engineering is still very rare. CAA techniques are hybrid methods requiring CFD calculations from which acoustical source information is extracted and fed into an acoustical solver. For rotating fluid machinery, acoustical investigations have been carried out mostly by semi-numerical methods based on simplified geometries such as profile cascades instead of an entire machine. The aim of the acoustic research of the Department of Fluid Machinery at the University of Karlsruhe, is to develop a CAA tool for noise prediction of fluid machinery in industrial applications. For the far-field acoustics, where reflections and refractions of the acoustic waves are negligible, a hybrid method using the Ffowcs-Williams/Hawkings acoustic analogy for the acoustic prediction serves very well even for complex, non-simplified 3D rotating fluid machinery. This is due to less demanding computational effort of the acoustical part compared to CAA field methods, whereas the CFD calculation of the rotating machinery is highly accurate due to the use of a fully 3D, unsteady large eddy simulation (LES).

In order to validate the in-house numerical acoustics tool and to investigate the effect of numerical models on acoustic predictions the noise of a simplified propeller with two (flat) blades of different inclination angles was investigated. The results for a 60° blade inclination angle are shown in Figs. 3–5. The LES was carried out in the fully 3D, rotating computational domain with a Reynolds number based on the tip velocity and the chord length of about 130,000. The experiments were carried out in the acoustic laboratory of KSB GmbH, Frankenthal, Germany. The numerical prediction of the sound pressure level agrees well with the experiment even in a coarse LES grid 5×10^6 control volumes.

[by I. Pantle, E. Sorgüven, F. Magagnato, M. Gabi, University of Karlsruhe, Germany]

2.4. Active control of buzz-saw tones

As part of the European SILENCER project, an experimental rig has been constructed aimed at the implementing a real-time active system for the control of a single low-order spinning mode ($m = 3$) in a no-flow duct. The rig is designed to simulate the characteristics of low-engine order buzz-saw modes. The mode was generated by the mode synthesiser ring shown in Fig. 6. A real-time single-frequency FXLMS controller was used to minimize the sum of the squared pressures at a single ring of seven error sensors using seven control actuators. In order to assess the performance of the control system the sound power flowing across the 'inlet' termination was measured using an intensity probe both before and after control. A comparison between measured and predicted sound power reductions versus frequency is shown in Fig. 7. The predictions were obtained using a primary field obtained the measured modal amplitudes before control, with the vertical lines corresponding to uncertainty in the radial mode amplitude of the $m = 0$ modes.

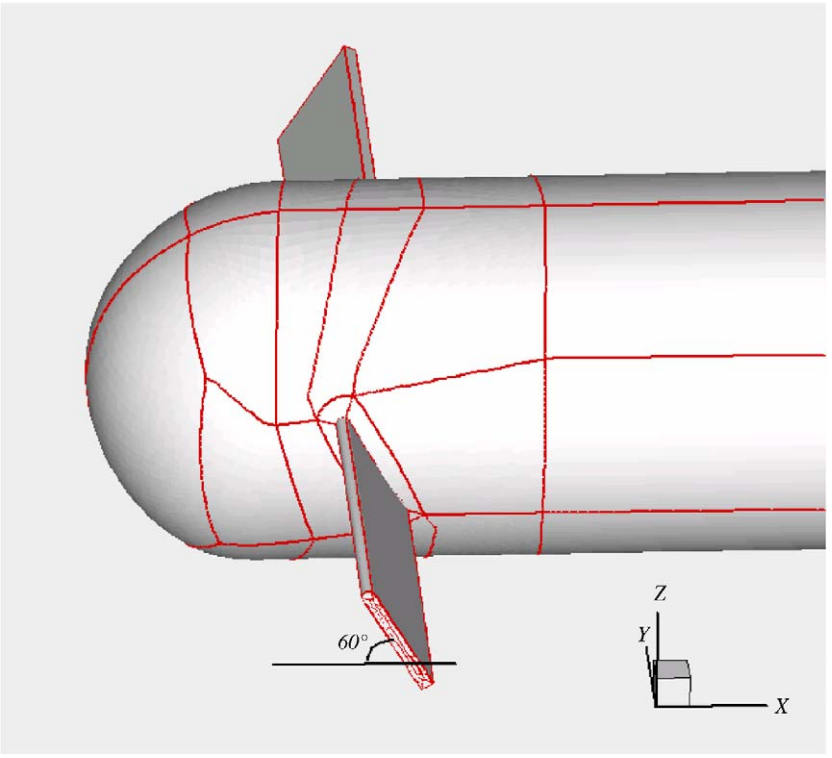

Fig. 3. Propeller geometry for LES (block boundaries of block-structured grid on surface).

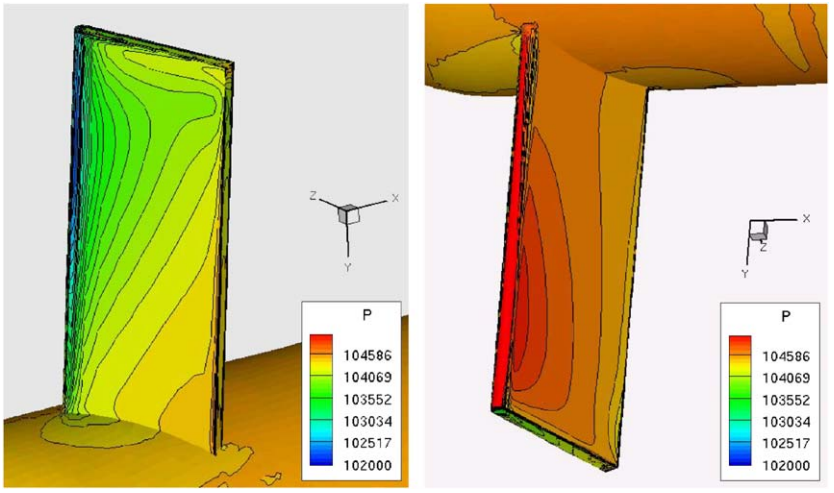

Fig. 4. Snap shot of pressure distribution on the blade (left: suction side, right: pressure side).

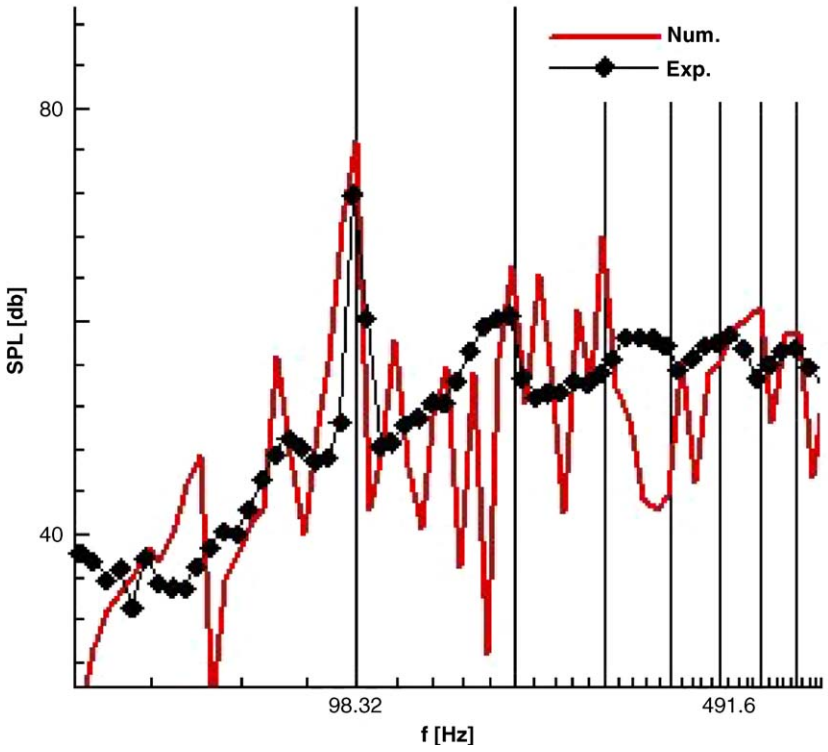

Fig. 5. Experimental and numerical sound pressure levels; blade angle 60°.

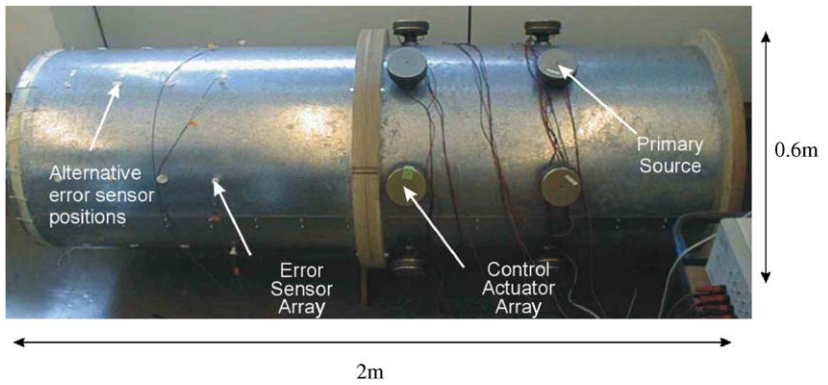

Fig. 6. Duct rig used in the active control of low-frequency spinning modes.

Reductions in sound power of up to 14.5 dB are measured following control. Theoretical predictions obtained are observed to overestimate the measured reductions. This may be due to the fact that the model assumes the pressure is driven perfectly to zero at the error sensors and that the walls are not perfectly rigid, as assumed in theoretical model. Some noise may therefore 'breakout' and re-radiate from the duct walls.

[by M. Wilkinson and P. Joseph, ISVR, University of Southampton, UK]

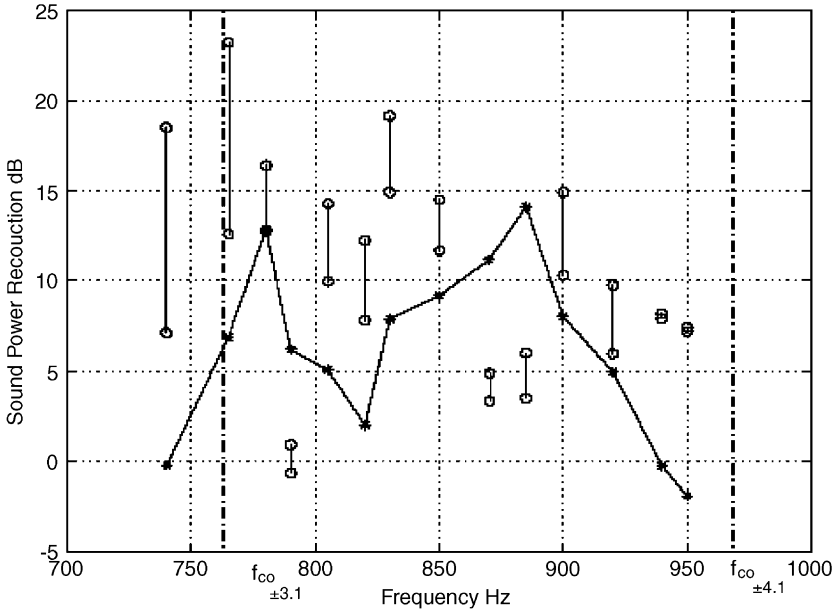

Fig. 7. Comparison between measured (solid line) and predicted sound power reductions.

2.5. An inverse method to predict spinning modes radiated by a turbofan

Deducing the modal structure generated by a ducted fan at a given acoustic frequency using only conventional free-field measurements is an interesting challenge because this would avoid direct modal analysis which is tedious and expensive. The proposed method to solve this inverse problem is based on the analytical equations governing ducted sound propagation and free-field radiation [1]. It leads to fast computations checked on Rolls–Royce tests made in the framework of previous European projects.

Results seem to be reliable although the system of equations to be solved is generally underdetermined as there are many more propagating modes than acoustic measurements. A limited number of modes are thus selected according to any a priori knowledge of the sources and a constrained iterative least squares fitting gives the final solution. An example is displayed in Fig. 8, and shows that eight modes (m, μ) out of the 83 propagating modes can duplicate the test data with an accuracy better than 1 dB at all the angles (m is the circumferential wavenumber and μ is the radial mode). A simple correction can be made at high speed to take account of the mean flow velocity inside the nacelle. It consists in modifying the actual frequency to keep the cut-off ratios unchanged and this shifts the directivity patterns.

This procedure will be implemented during the model engine fan tests planned within the EU SILENCER project and will include both in-duct modal analyses and free-field acoustic measurements. The objective is to provide input data for the prediction of noise radiation in other configurations for the optimisation of duct linings.

[by S. Lewy, ONERA, Chatillon, France]

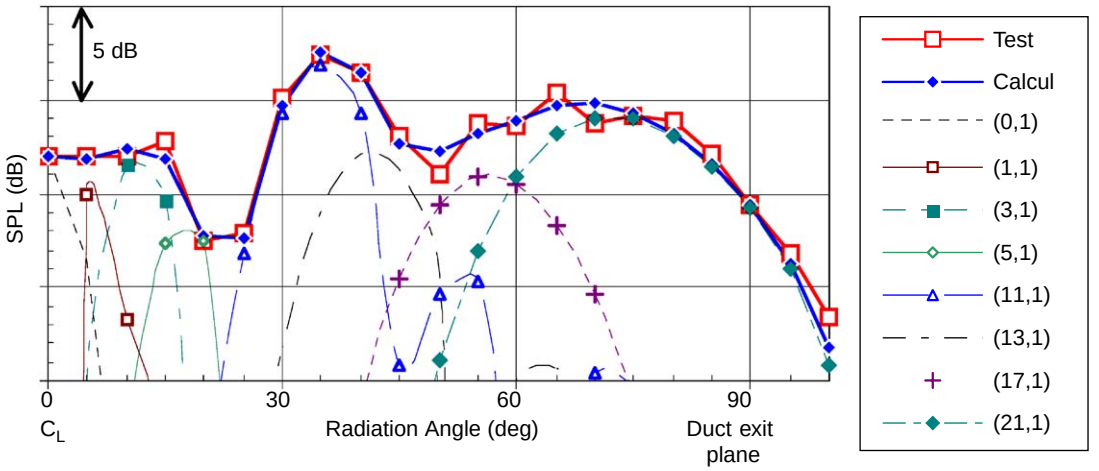

Fig. 8. Sound pressure level (SPL) radiated upstream of RESOUND fan LNR1 ($D = 0.864$ m; Rotation speed = 7013 rpm; Blade pass frequency = 3039 Hz).

3. Jet noise

3.1. Jet noise predictions—JEAN

The objectives of Jet Exhaust Aerodynamics & Noise (JEAN) project funded under the 5th Framework programme of the EU were to develop and assess methodologies for the prediction of noise generated by high-speed subsonic jets. An experimental programme was conducted at the Martel facility at CEAT, Poitiers to provide a database for the validation of the aerodynamic and acoustic prediction techniques. Laser Doppler anemometry was used for extensive aerodynamic measurements for both hot and cold jet conditions. Both near field and far-field acoustic data were also acquired and used to benchmark the noise prediction methods.

CFD techniques for prediction of the aerodynamic characteristics of jets were further developed. Industry standard techniques using Reynolds averaged Navier Stokes equations (RANS) were assessed and updated and new developments were undertaken which used vortex filament methods (VFM) and LES. A detailed comparison of the CFD predictions with the experimental data was undertaken and both the time averaged results (mean, mean square) and the time-dependent results (auto & cross spectra, length & time scales) were considered. From this, it was concluded that the RANS procedures provided better estimates of the both the magnitudes and spatial variation of the mean quantities with the main drawback the assumption of isotropy in many of the codes. The LES procedures underestimated the length of the potential core and overestimated some turbulence statistical properties short of the potential core. The spectra from LES data were in reasonable agreement with the experimental data but the resolution of the LES spectra at higher frequencies was poor although the experimental data were also liable to errors at the higher frequencies. The correlation lengths, time scales and convection

speeds determined from the LES procedures were generally in good agreement with the experimentally derived values.

Noise source and propagation models were also developed and benchmarked. Techniques used included the acoustic analogy based both on statistical methods using k–ε CFD computations and on a vorticity-source formulation using LES computations, SNGR approaches based on a stochastic modelling of the source term (from k–ε CFD) and propagation of acoustic waves into the far field via LEE or a combination of LEE and Kirchhoff integral. Further techniques included LES computations in the flow for the near field, which were extrapolated to the far-field using both the Kirchhoff and Ffowcs-Williams/Hawkings formulations and "Acoustic LES" where the acoustic field was obtained at the same time as the flow field. The combination of LES with a Kirchhoff procedure based on a surface parallel to the jet development profile enabled predictions within 3 dB of the measured directivity level.

[by J. Fitzpatrick, Trinity College, Dublin, Ireland]

3.2. Comparison of jet noise prediction methods

Several hot jet configurations were computed and compared by means of a hybrid LES/CFD using an acoustic integral surface formulation. This multi-code approach has been applied to realistic configurations of hot jets, representative of actual jets of industrial interest. The jet Reynolds numbers, which were in excess of 500,000 were not artificially reduced. In order to ease the treatment of inflow boundary conditions it was decided to include the nozzle in the computation, although the boundary layers inside the nozzle could not be properly resolved. The grid size penalty implied by including a nozzle domain in the computational domain was compensated by the fact that no external forcing procedure was required to destabilize the jet flow. This approach, although successful in providing realistic unsteady jet flows, had some drawbacks, the most visible being a consistently shorter potential cone with respect to available measurements and a systematic over estimation of far-field sound pressure levels. Work is in progress to resolve these discrepancies. Nonetheless, the results from this approach can be compared to different acoustic post-processing methods. In particular, in the case of hot jets, it was demonstrated that the Ffowcs-Williams/Hawkings approach was better suited that the more classical Kirchhoff method [2]. The characteristics of the jets under consideration are listed in Table 1.

The computed far-field sound pressure levels were compared to the measurements in a relative way as shown in Fig. 9. Although the method was found to overestimate the absolute levels, the relative comparisons demonstrated that the simulations are able to correctly predict the large changes in the directivity pattern associated with the different jet conditions [3]. This will be of great importance when assessing the benefits of noise reducing devices or nozzle arrangements.

[by F. Vuillot, G. Rahier, N. Lupoglazoff, J. Prieur, A. Biancherin, F. Muller, ONERA/DSNA]

3.3. Direct coupling between large eddy simulations and finite-element computations of Lighthill's analogy

The complexity of CAA is mainly due to length scale disparities between the fluid dynamics and the acoustics. For most problems the domain required for the flow computation is quite small

Table 1
Jet characteristics

	R_{obs}	D (10^{-3} m)	M_j	U_{jet} (m s^{-1})	T_i (K)	$Mc = \frac{U_j}{c_j + c_a}$	$M'_c = \frac{U_j + c_j}{c_j + c_a}$	$M_e = \frac{U_j}{c_a}$
Seiner & Ponton	40D	91.44	2	1120	1370	1.25	1.87	3.3
ONERA	75D	80	0.7	410	900	0.45	1.07	1.2
ONERA "Froid"	75D	80	0.7	230	307	0.35	0.85	0.7
TANNA	72D	50.8	0.87	325	400	0.46	0.98	0.96
TANNA TP19	72D	50.8	0.75	310	468.7	0.41	0.95	0.89

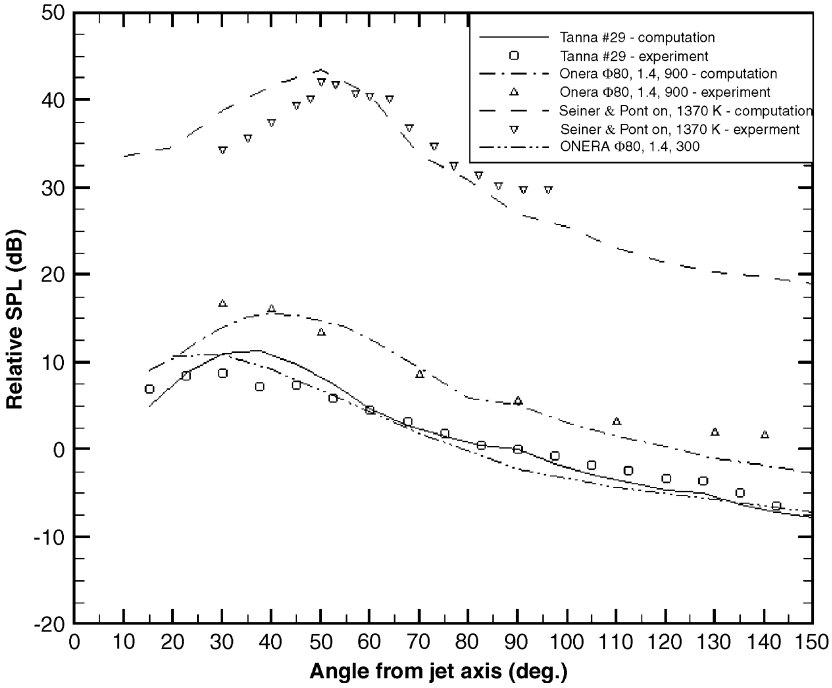

Fig. 9. Relative comparisons of predicted & measured far-field SPL (observation distance: 75D; reference value: Tanna at 90°).

compared to that for the acoustic computation. However, the domain discretization for the fluid dynamics has to be much finer than for the acoustics. A coupling scheme, which offers for both physical fields different meshes and which uses MpCCI for the data exchange between these meshes has been developed. The flow is computed by LES using a fully conservative second-order finite-volume space discretization and a pressure correction method of the SIMPLE type. The computation of the generated noise is performed using a finite-element method, which solves the inhomogeneous wave equation of Lighthill's acoustic analogy. The setup for the computation of

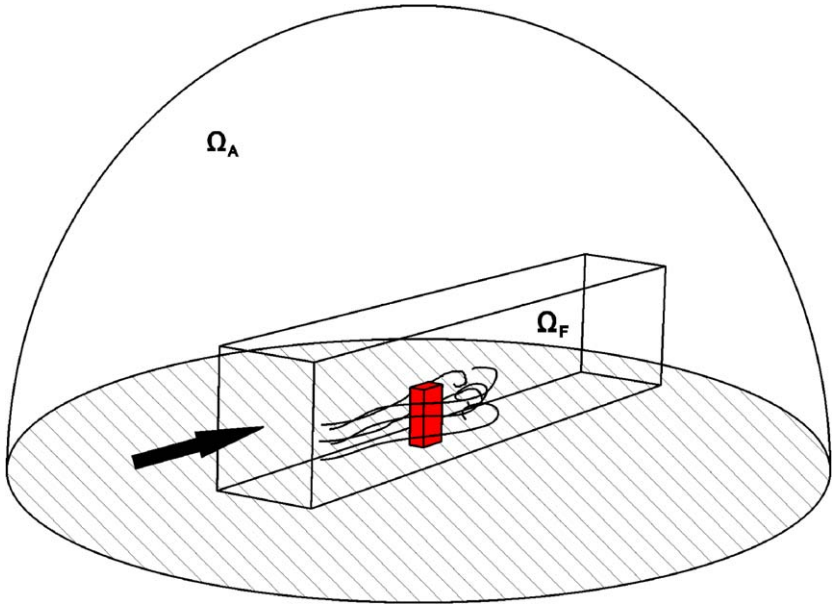

Fig. 10. Geometric set-up.

the acoustic noise generated by a flow around a square cylinder is shown in Fig. 10. The computed acoustic field for a cross section is given in Fig. 11 and it can be clearly seen that the sound field corresponds to that of a dipole as can also be seen in the directivity pattern of Fig. 12. The frequency spectra of the acoustic pressure is shown in Fig. 13, where p_1 is a pressure in the turbulent region of the flow and p_2 a pressure in the far field. The acoustic pressures in the far field compare well with measured data.

[by M. Kaltenbacher, S. Becker, M. Escobar, A. Irfan, R. Lerch, F.Durst, University of Erlangen]

3.4. Jet geometric near field prediction for acoustic loads

Traditionally, theoretical and semi-empirical methods for jet-noise prediction have concentrated on the far field where the effects of the spatial extent of jet-noise source are not present. However, to estimate the acoustic loadings on airframes these effects have to be taken into account. A semi-empirical model for the prediction of jet noise in the geometric near field that incorporates effects due to the spatially extended nature of the jet sources has been developed. The four source method of Fisher and Preston [4,5], originally devised for the prediction of far-field noise of simple coaxial jets, has been extended to the geometric near field by allowing for an axial distribution of noise sources. A method for predicting the axial distribution of the jet-noise source strength for a coaxial jet has been developed and incorporated in the model. A new method to extrapolate the far-field directivity of simple coaxial jets has been included in the model to enlarge the area in which the noise prediction is possible. The latter model is based on the geometric-

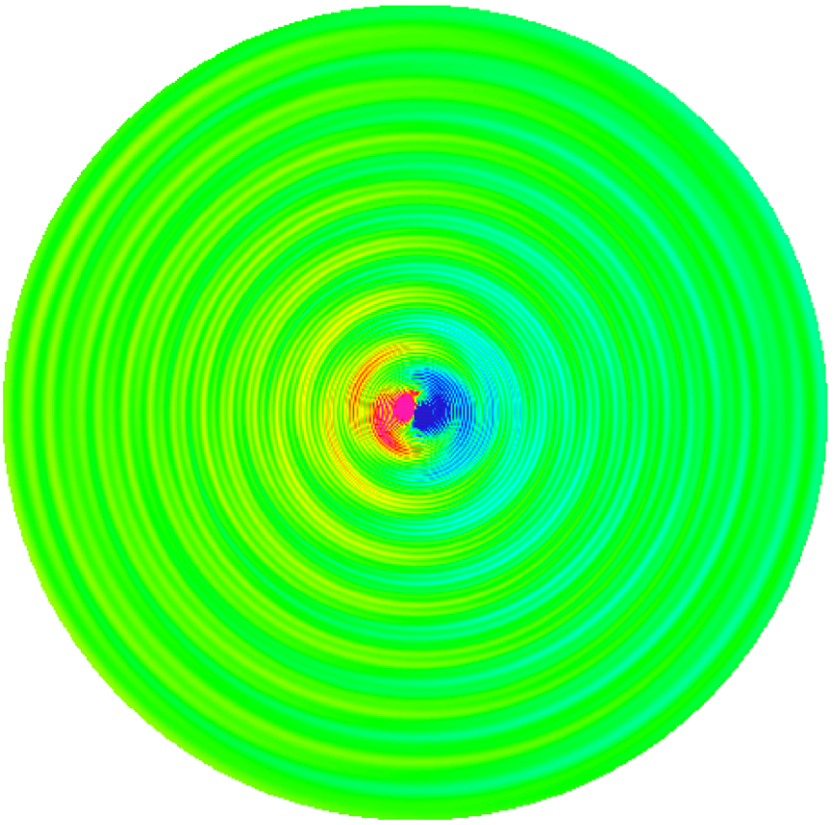

Fig. 11. Acoustic sound field.

acoustics scaling laws proposed by Morfey et al. [6]. Comparisons between the model and a limited set of 1/3-octave data measured on the skin panels of two commercial aircraft show encouraging agreement as can be seen from Figs. 14 and 15. The geometric near field prediction scheme can be extended to estimate simple installation effects including reflections on prescribed surfaces and to evaluate geometric near-field effects on measured jet-noise spectra.

(by A. Bassetti, ISVR, University of Southampton, UK)

4. Duct acoustics

4.1. Cut-on, cut-off transition in aircraft engine ducts

The phenomenon of cut-on cut-off transition of acoustic modes in ducts with mean flow has been examined using an analytical multiple-scales solution and the results compared to solutions obtained from a numerical finite-element method [7]. The analytical solution, derived by Ovenden

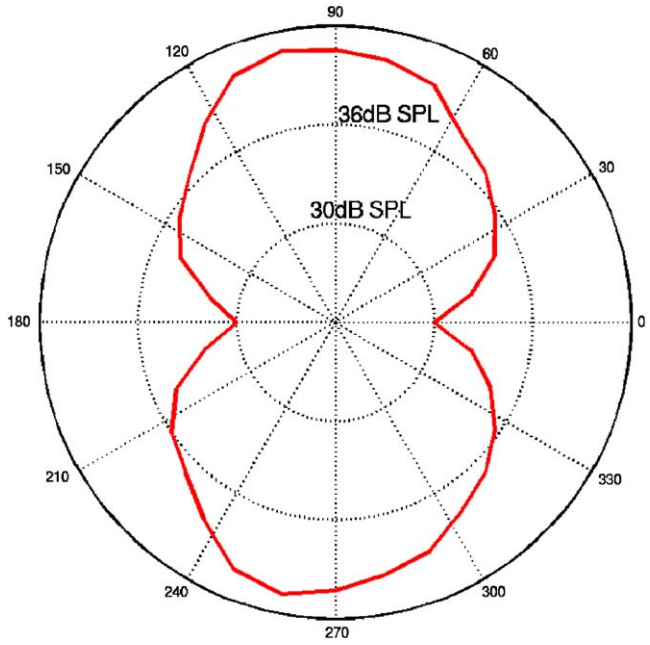

Fig. 12. Directivity pattern of far field.

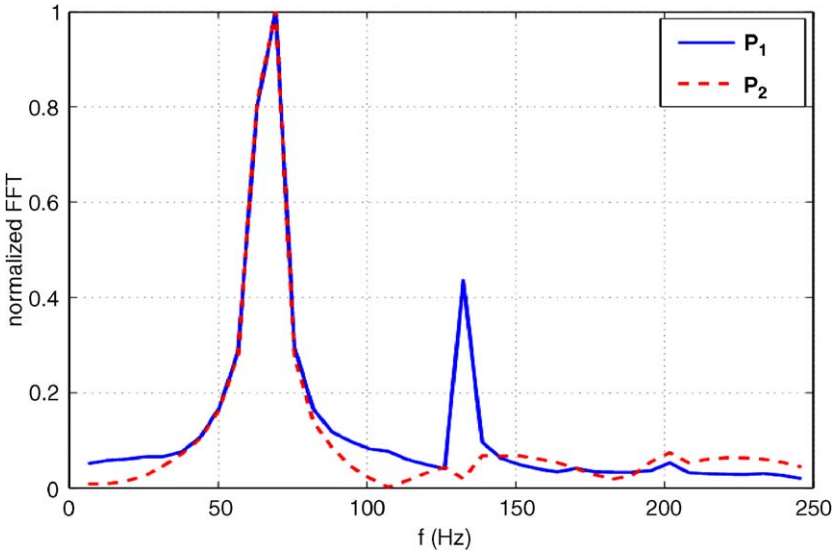

Fig. 13. Frequency spectra of acoustic pressure.

[8] for an arbitrary duct with irrotational mean flow, encompasses the inner boundary-layer solution in the neighbourhood of the transition point and the outer slowly varying modal solution far upstream and downstream. Test cases for a geometry representative of a high-bypass turbofan

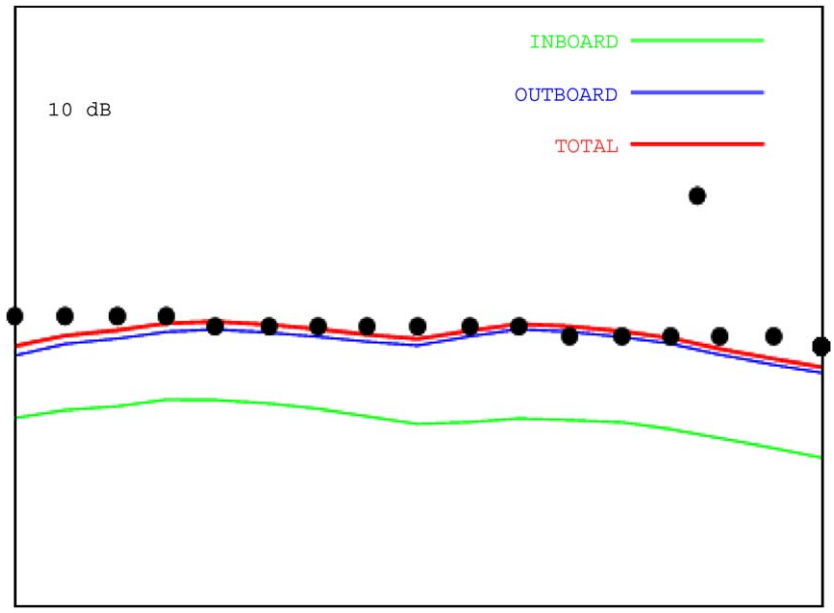

Fig. 14. Octave spectrum (1/3) measured on the left-wing aileron of a four engined aircraft (bullet) and predicted jet noise spectrum (red line). (Green & blue lines show the separate contributions to the total predicted spectrum from the left-wing engines.)

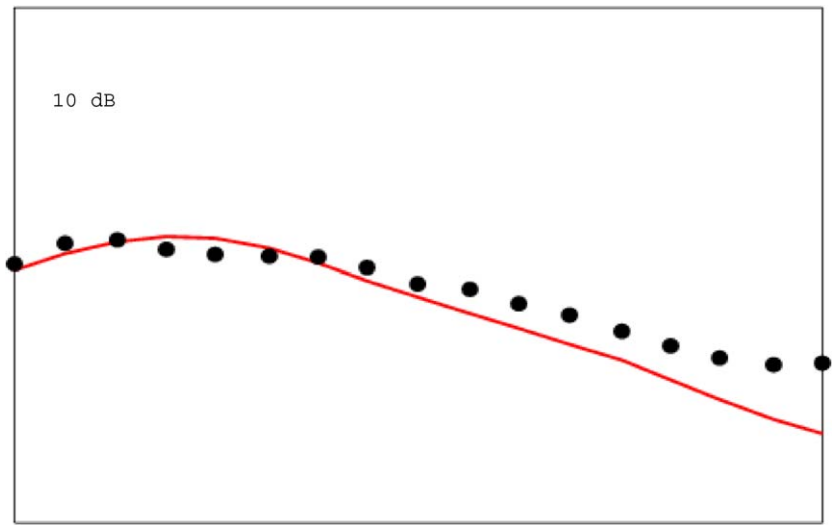

Fig. 15. 1/3 octave spectrum measured on the left side of the fin of a two engined aircraft (bullet) and predicted jet noise spectrum emitted from the left-wing engine (red line).

engine span a realistic range of frequencies and circumferential mode numbers. The agreement is in most cases remarkably good as shown in Fig. 16. The solution should enable designers to continue to use multiple-scales methods to examine flow pressure and noise transmission inside an

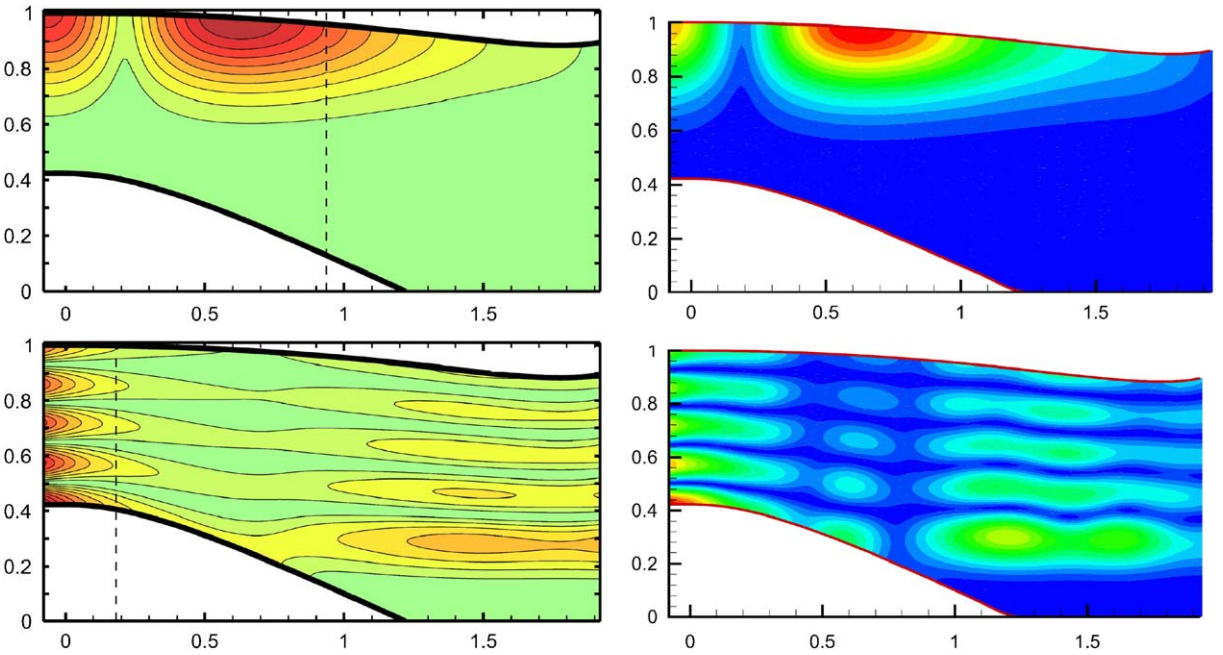

Fig. 16. Multiple scales (left) and FEM (right)—Mach no. = 0.5 Top: 1st radial mode with $m = 10$ and $\omega = 11$ Below: 5th radial mode with $m = 5$ and $\omega = 19.8$.

engine duct with the capacity to include directly the contributions of modes undergoing transition without encountering singular behaviour.

[by N.C. Ovenden, UCL, UK & S.W. Rienstra, TUE, Netherlands]

4.2. *Plane wave decomposition using microphone arrays in ducts*

A general plane wave decomposition procedure that determines both the wave amplitudes or the reflection coefficient and the wavenumbers is proposed for in duct measurements. To improve the quality of the procedure over determination and a nonlinear least-square procedure is used. The procedure has been tested using a six microphone array and used for accurate measurements of the radiation from an open unflanged pipe with flow. The experimental results for the reflection coefficient magnitude and the end correction have been compared with the model developed by Munt [9]. The agreement is very good if the maximum speed rather than the average is used to compare measurements and theory. This result is the first comprehensive comparison with the theory of Munt. The damping of the plane wave (the imaginary part of the wavenumbers) could also be obtained from the experimental data. It is found that the damping increase strongly, compared with the damping for a quiescent fluid, when the acoustic boundary layer becomes thicker than the viscous sub-layer. This finding is in agreement with a few earlier measurements and is also in agreement with a theoretical model proposed by Howe [10]. The results in Fig. 17 show that the model works well typically up to a normalized acoustic boundary layer thickness δ_A^+ of 30–40. For values of a δ_A^+ less than 10, corresponding to higher frequencies or lower flow

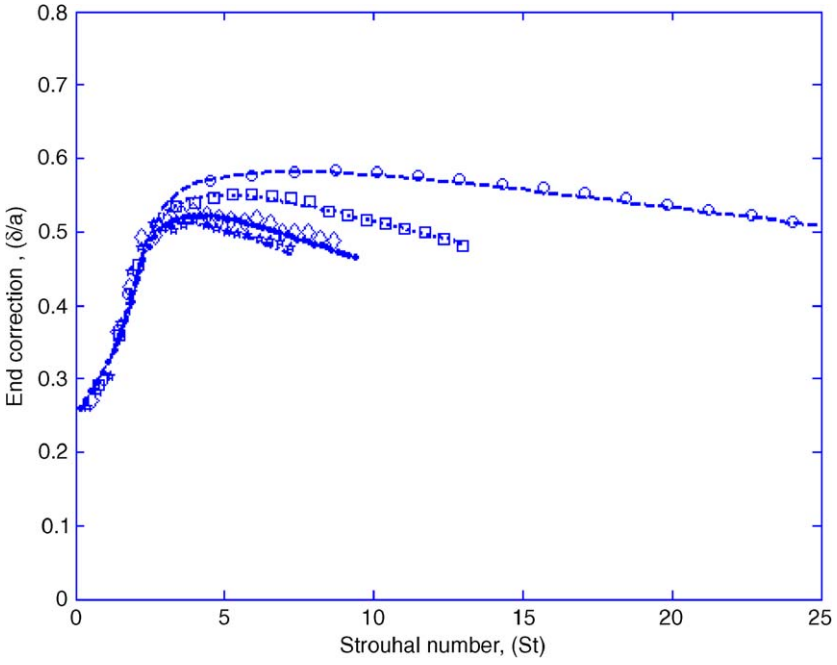

Fig. 17. Measured and predicted normalized end correction ○ ○ ○, Measured at $M = 0.05$, ––––, predicted at $M = 0.05$ by Munt [9]. □ □ □, Measured at $M = 0.10$, ..., predicted at $M = 0.10$ by Munt [9] ◇ ◇ ◇, Measured at $M = 0.15$, • • • •, predicted at $M = 0.15$ by Munt [9] ***, Measured at $M = 0.20$,–.–.–., predicted at $M = 0.20$ by Munt [9].

speeds, the model proposed by Dokumaci [11] was also in good agreement with the experimental data.

[S. Allam and M. Åbom, KTH, Sweden]

4.3. *Multi-modal propagation in ducts*

A multi-modal propagation method to study sound propagation in varying cross section lined ducts has been developed [12]. The wall impedance can be non-uniform in both axial and circumferential directions and the cross section can be slowly varying. Using the method, real turbofan duct problems can be easily addressed, even at high values of the reduced wavenumber $K = \omega/cR$, where R is the characteristic dimension of the duct. The wave propagation problem is transformed in a scattering problem as follows. The whole duct is decomposed into three contiguous regions with respect to axial coordinate z: left and right semi-infinite uniform rigid ducts connected by an arbitrarily varying cross section transition lined region. The sound pressure and axial particle velocity are projected on the local rigid modes, which are known a priori. This projection corresponds to the exact decomposition in the uniform rigid regions and provides a coupled representation of the total wave field in the transition region. The direct integration of the Helmholtz propagation equation can lead to

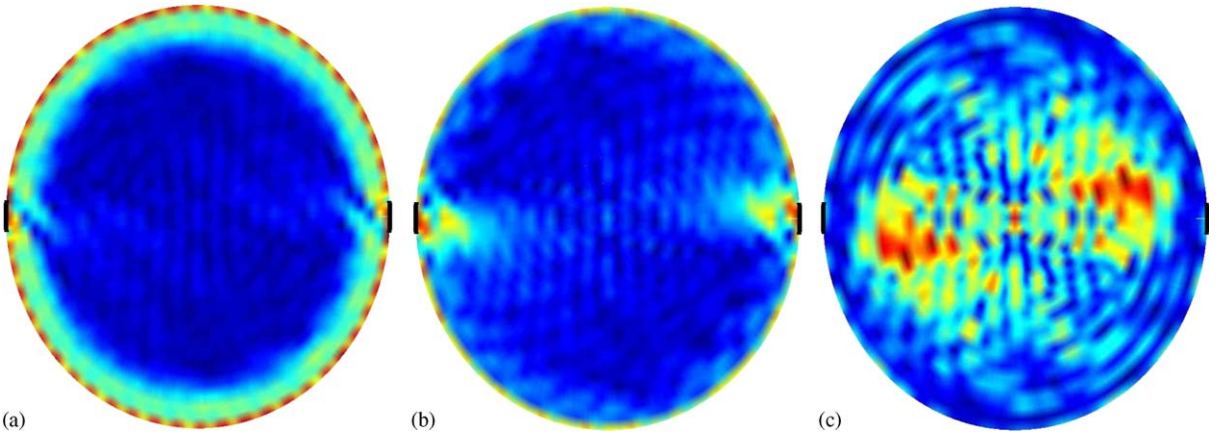

Fig. 18. Pressure magnitude for the incident mode (26,0) $K = 31.26$; lined wall of reduced impedance = 2-j with two hard-wall splices axial position: (a) $z = 0.01$ R, (b) $z = 0.2$ R, (c) $z = 0.5$ R.

instabilities. By introducing the modal impedance Z and an additional transmission operator T, two stable equations are obtained. These two differential matrix equations are integrated simultaneously from the free end to the source plane. The memory requirement for this calculation is of $O(N^2)$ where N is the number of modes considered. This is much less than $O(N^2 \times Nz)$ where Nz refers to the number of steps of the axial discretization used in the more classical methods like FEM. Some results are shown in Fig. 18. With this method, all modal coefficients for reflection and transmission of the overall transition lined region are obtained so that only one calculation is needed for any source configuration. This method ensures energy conservation when the liner is not dissipative and could be generalized to account for the presence of flow.

(by W.P. Bi, V. Pagneux, D. Lafarge & Y. Aurégan, LAUM, Le Mans, France)

5. Airframe noise

5.1. Acoustic resonances in a high lift configuration

Acoustic resonances in open systems have been computed by Hein et al. [13] using perfectly matched layer (PML) absorbing boundary conditions in the form of the complex scaling method of atomic and molecular physics. Application of the technique to resonances in rectangular open cavities by Koch [14] has shown that tonal noise can be enhanced by such resonances. Tonal noise is also a problem in high lift configurations for aircraft landing and approach. Computations were also performed for acoustic resonances in a generic two-dimensional high lift device. These resonances turned were identified as surface standing waves by Hein et al. [15] and agreed quite well with the experimentally observed low-frequency tones of a half-span model as reported by Pott-Pollenske et al. [16]. A comparison of the computed resonances (left) with the

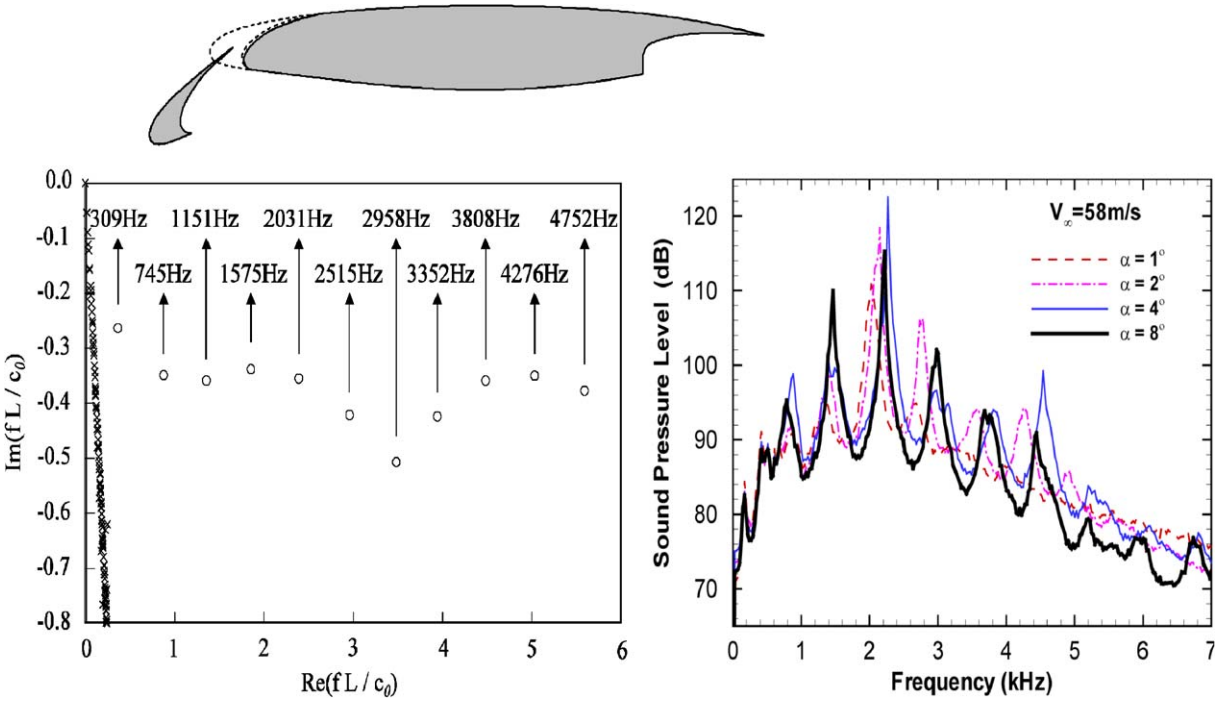

Fig. 19. Comparison of computed resonances with experimental results [16].

observed tonal frequencies (right) of a high lift configuration with a slat but without a flap is given in Fig. 19.

[by S. Hein, W. Koch and J. Schöberl, DLR, Germany]

5.2. *Gear-wake/flap interaction noise*

Acoustic wind tunnel tests have been carried out on a 1:13 scaled 2D wing section with generic main landing gear. An out-of-flow microphone array was used to localize and quantify different noise sources, while directivity was measured with farfield microphones. Tested configurations included closed/open cavity, with/without wheels and varying gear position. Interaction noise was reduced by a porous flap leading edge and flexible brushes at the main wing trailing edge. Results shown in Fig. 20 clearly indicate the presence of interaction noise, radiated from the flap leading edge, which is most pronounced at low frequencies, where it dominates the noise from the landing gear itself. The interaction noise shows no pronounced radiation directivity or dependence on angle of attack, except for a low frequency forward arc radiation. The noise levels scale with U^6 as a function of Strouhal number. The gear rather than the cavity contributes most to the turbulent wake impinging on the flap. Positioning the gear further upstream results in a reduction of interaction noise of a few dB. Larger reductions may be

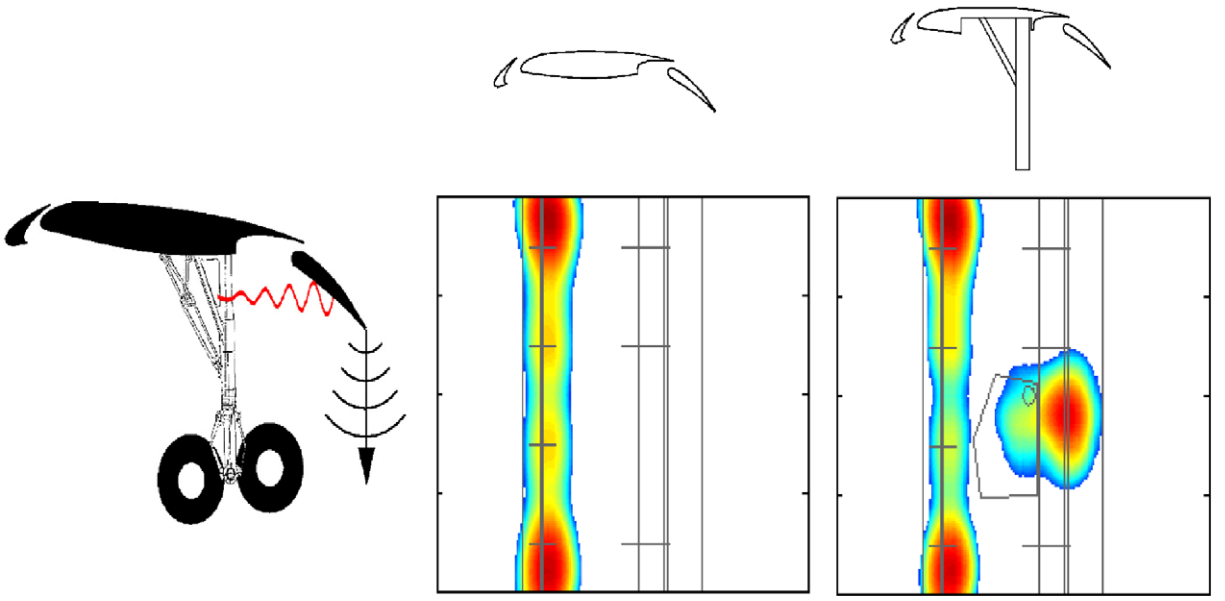

Fig. 20. Sketch of gear-wake/flap (left) interaction noise mechanism and acoustic source plots without (middle) and with (right) generic landing gear.

obtained with a porous flap leading edge. This work was conducted as part of the European SILENCER program.

[by S. Oerlemans, NLR, Netherlands & M. Pott-Pollenske, DLR, Germany]

5.3. *Design and testing of low noise landing gears*

In the approach phase of large commercial aircraft flow noise from landing gears significantly contribute to overall aircraft noise. A study in low noise landing gear design was performed to develop operational landing gears, which take into account aeroacoustic constraints early in the design stage within the EU SILENCER project. Airbus A340 type gears were selected as the reference. RANS flow field calculations were performed to identify and thus avoid the impingement of high-speed flow onto critical gear structure elements. The evaluation of the CFD results with respect to the effects on aerodynamic noise were performed on the basis of related experimental experience. Both low noise advanced nose and main landing gears were designed and manufactured at full scale for noise testing in the $8\,\mathrm{m} \times 6\,\mathrm{m}$ open test section of the German-Dutch Wind Tunnel (DNW-LLF). Relative to the conventional reference gears a reduction of broadband landing gear noise in the order of 5–7 dB was achieved. A comparison of the noise spectra obtained for the A340 reference nose landing gear (NLG) with the same gear with streamlined fairings attached (RAIN project) and with the SILENCER advanced low noise NLG is shown in Fig. 21.

[by W. Dobrzynski, DLR, Germany]

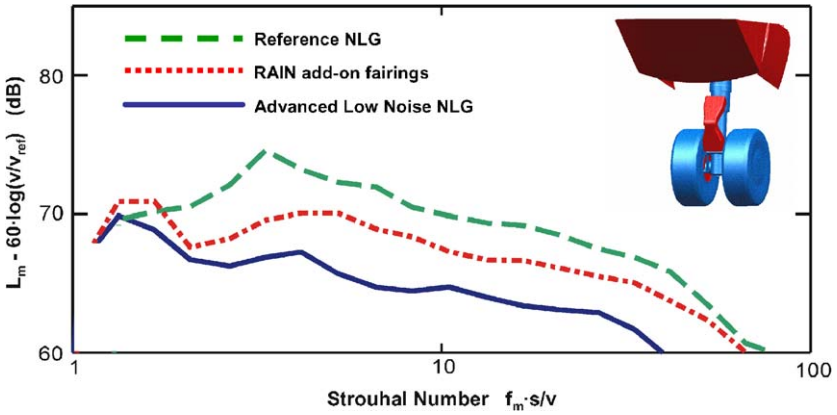

Fig. 21. Example of noise reduction as achieved for the advanced nose landing gear.

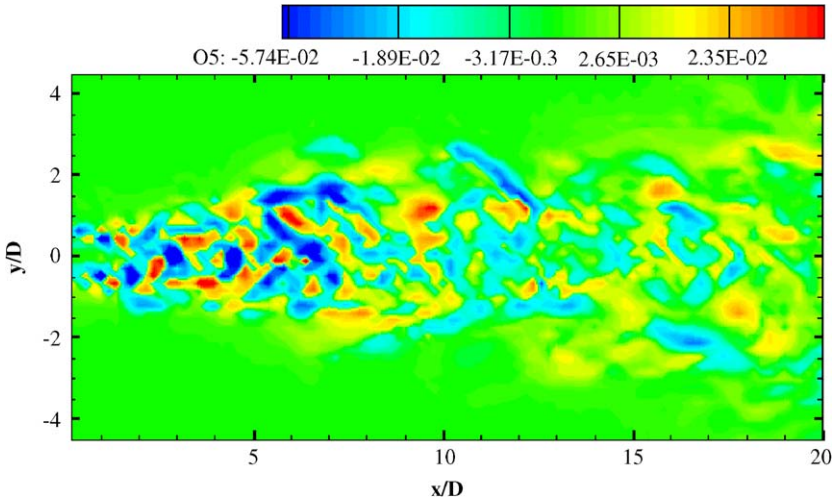

Fig. 22. Contours of the total time derivative of the density within the HD-flame in streamwise direction.

6. Combustion noise

6.1. Perturbation methods for combustion noise simulation

Combustion noise from open non-premixed flames has been simulated with a hybrid method in which incompressible LES was used for the fluid mechanics while the acoustic simulation used acoustic perturbation equations (APE) proposed by Ewert and Schröder [17,18]. It is known from theoretical analysis that combustion noise is dominated by heat release effects accompanied by entropy fluctuations. Unlike formulations where the entropy contribution is neglected, the entropy source is taken into account as it represents a major contribution to combustion

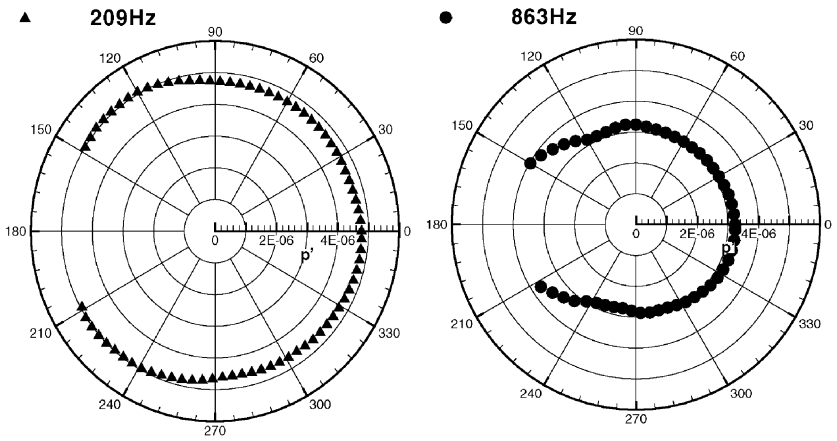

Fig. 23. Directivity patterns for different frequencies. Center point at $(x, y.z) = (10, 0, 0)$ and radius $r/D = 17$.

generated noise. Based on the conservation equations for reacting flows an APE-System was derived. The left-hand side is identical to the APE-2 System [18] to take advantage of its stability properties, while the right-hand side (RHS) consists of all other nonlinear terms including the heat release effects. This extended APE-System is particularly suitable to identify and analyse the different source terms and their influence on the radiated sound field of reacting flows. The contours of the density fluctuation within the flame, which generate the acoustic pressure field are illustrated in the streamwise centre plane in Fig. 22. The directivity patterns of Fig. 23 show the monopole character of the flame caused by unsteady heat release at two different frequencies.

[by T.Ph. Bui, M. Meinke, W. Schröder, RWTH Aachen, Germany]

7. Helicopter noise

7.1. Flight procedure design for helicopter noise abatement

The flyover noise of helicopters varies with flight conditions, such as flight speed and flight path angle. As a first step towards a helicopter noise abatement flight procedure design, the techniques for rotorcraft noise ground footprint prediction, using either purely numerical computations or measured sound fields on limited microphones have been developed at DLR. The numerical computations for noise footprints consist of a combination of the DLR 3D free wake code, the UPM-Mantic code [19], a Ffowcs-Williams/Hawkings-based code APSIM together with a flyover noise prediction code, Hemisphere. The footprints can be used to evaluate noise reduction of different flight procedure. Fig. 24 shows the predicted EPNL ground footprint compared with a flight test result. The comparison demonstrates similar characteristics for both noise levels and directivity patterns. Methods for low noise flight procedure design can be fulfilled by above-mentioned two techniques. For a quick estimation of flyover noise reduction, acoustic data from a flight test are used together with the DLR Hemisphere code. The noise abatement flight procedures for different segment of flight trajectories and descent angles were tested and

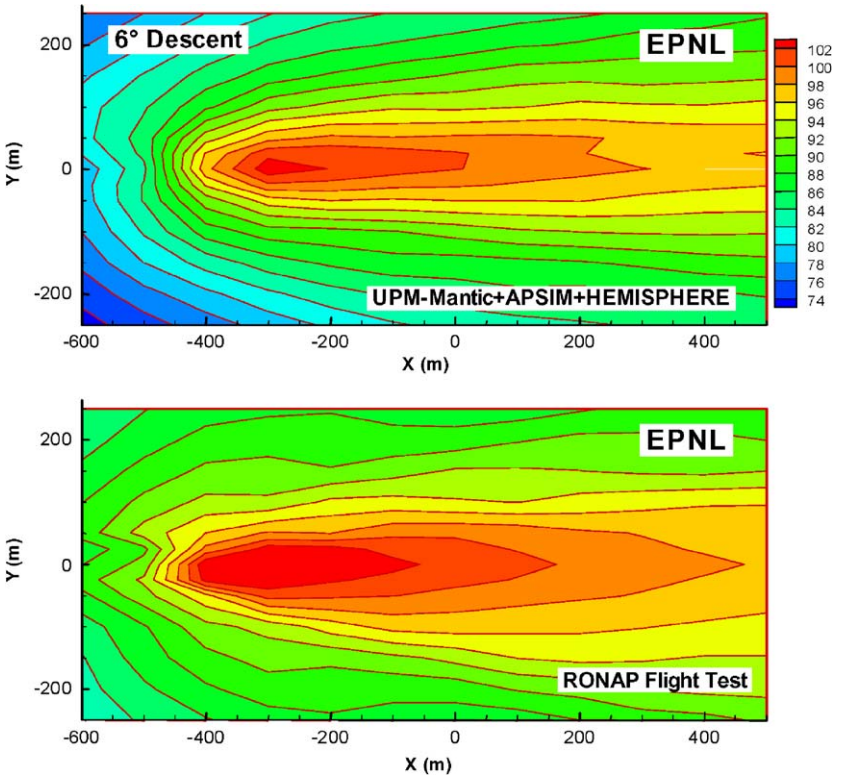

Fig. 24. Comparison of predicted EPNL ground footprint with flight test result.

compared with a reference of a 9° descent flight (Maximum BVI noise case). Fig. 25 shows two designed noise abatement procedures (MS1 and MS2) for descent flight and their comparison with a normal 9° descent flight. Compared with footprints of 9° approach, Fig. 26 clearly illustrates that the multi-segment noise abatement procedures are effective and provide clear evidence that approach noise reductions are achievable.

[by Jianping Yin, DLR, Braunschweig, Germany]

8. Aircraft interior noise

8.1. Optimized sound absorbing panels with quarter-wave resonators

In order to reduce aircraft interior noise, sound absorbing trim panels have been designed based on tube resonators of different lengths and diameter, allowing optimization of the absorption characteristics along a frequency range [20]. The trim panel consists of an array of identical characteristic areas as shown in Fig. 27. The absorption coefficient of an optimized sample, measured in an impedance tube, is shown in Fig. 28 together with the results from two samples with the same, but differently distributed, resonators. The resonator was optimised for maximum

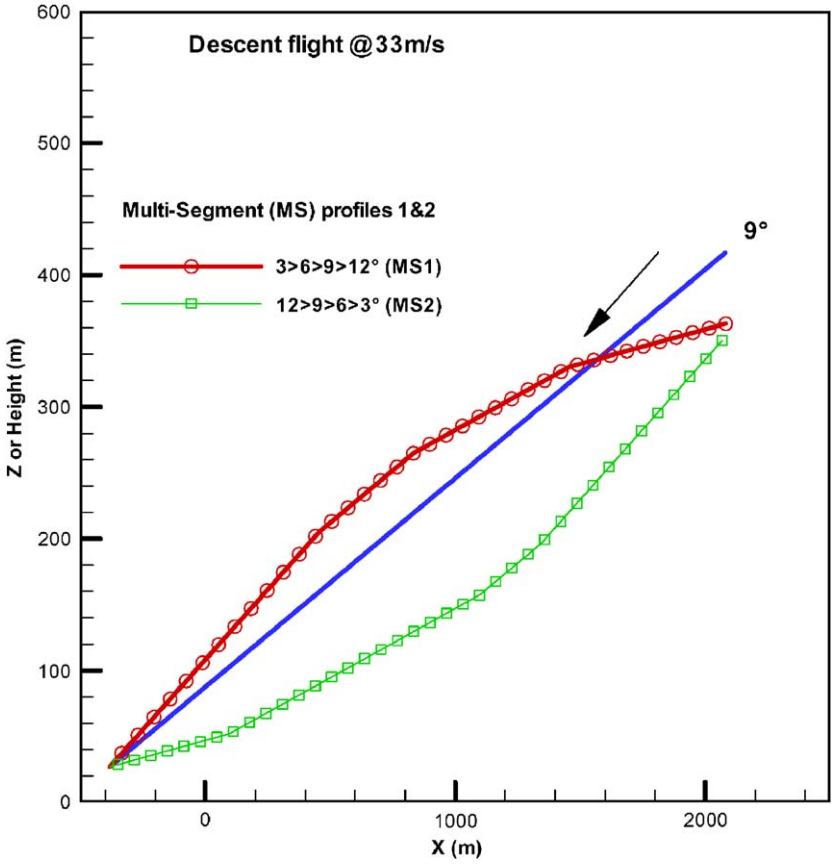

Fig. 25. Description of two Multi-segmented approach profiles.

sound absorption within 1000–2000 Hz. Very high absorption levels are obtained and agree well with theory. The work has been performed within EU project Friendly Aircraft Cabin Environment (FACE).

[by M.H.C. Hannink, Y.H. Wijnant & A. de Boer, University of Twente, Netherlands]

9. Techniques and methods in aeroacoustics

9.1. Object-oriented methods for aeroacoustic predictions

The integral methods based on Lighthill's acoustic analogy, such as the Ffowcs-Williams/Hawkings equation, the Kirchhoff formulation and the Porous (or Permeable) Ffowcs-Williams/Hawkings equations, are well suited for object-oriented (OO) structures. The solution of surface or volume integrals required by these methods can be efficiently performed by having each panel on the body or on the control surface and each cell in space as a separate object, capable of evaluating the integrals on itself and of storing the data in a flexible form that allows for fast

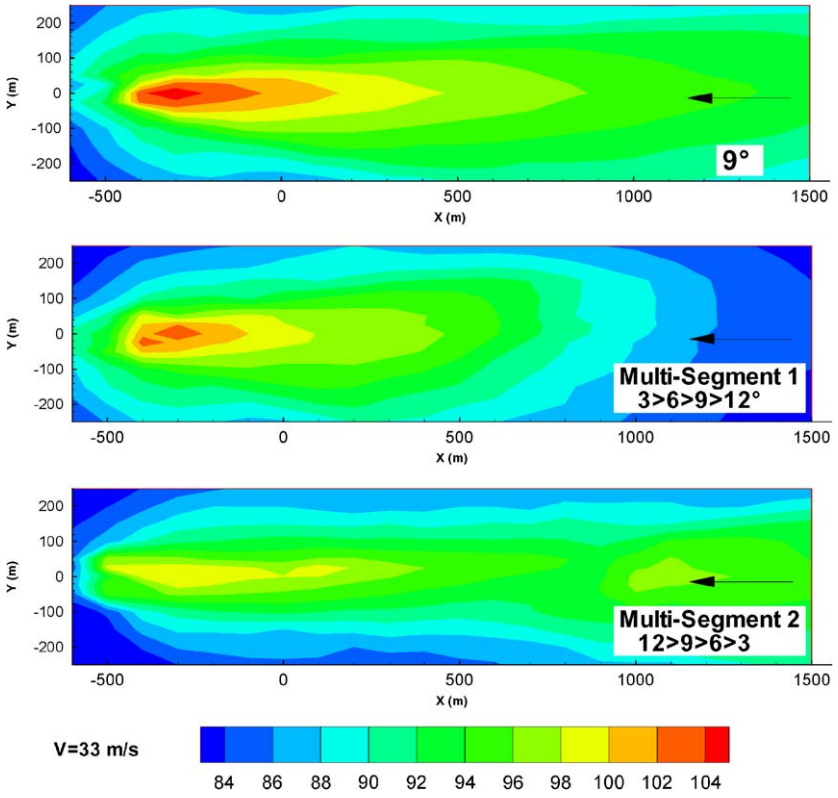

Fig. 26. EPNL ground footprint at multi-segment flight profiles at constant speed.

interpolation of the data. Through the use of an OO design it has been possible to obtain an "all-purpose" code that can be used for aeroacoustic analysis of an arbitrary unsteady flow field, with the possibility of a number of systems of reference in arbitrary motion. This is achieved by using an OO structure strongly based on abstract classes with the property of polymorphism, while the storage and successive interpolation of noise data is done dynamically and efficiently using container classes. As for the construction of the emission surface, it can be shown that the "marching cube" algorithm, a well-known computer graphics algorithm that is very efficient in evaluating iso-surfaces, integrates very well within the OO framework. The OO approach allows to gain a universal applicability of the integral methods, while maximizing the reuse of code among the different methods. The object model has been implemented in the form of a library, named Object-oriented Library for Aeroacoustics (OLA), to allow it to be called from conventional codes (not object oriented) without any knowledge of the internal object structure.

[by V. Botte, CIRA, Italy]

9.2. *Source location using matched field processing*

A method of source location developed by Battaner-Moro [21] utilizing signals acquired from an array of microphones analysed using polar correlation and matched field processing has been

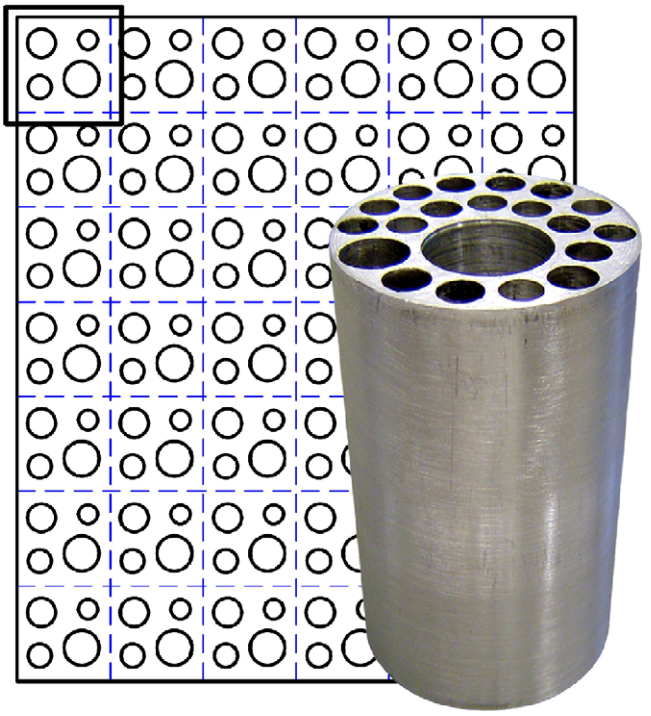

Fig. 27. Sample of characteristic absorber area.

successfully applied to a number of problems during 2004. Data for jets from model scale aircraft engine nozzles has been analysed to give jet source breakdowns that have contributed to the understanding of forced mixer technology. While jet noise remains the main application of the technique, theoretical enhancements have allowed the use of a novel 125 channel microphone array used to acquire data during the final testing phase of the SILENCER project and given source location data from five engine configurations that test new zero-splice intake and lip acoustic lining technologies.

[by J. Battaner-Moro, ISVR, University of Southapton, UK]

9.3. Acoustic source identification

Near-field pressure measurements can be used to determine the vibrational patterns of a radiating surface. The preferable method is the inverse frequency response function method (IFRF), because it is generally applicable and imposes no limitations on the shape of the measurement grid and the surface of the source. As the IFRF method requires inversion of an ill-conditioned system of equations, application of regularization (stabilization) techniques are required. An inverse boundary element method (IBEM), based on IFRF, has been developed to identify noise sources from a measured noise field. The measured data may be sound pressures from a conventional microphone or particle velocities from a new type of acoustic sensor (Microflown) developed at the University of Twente. Results show that, under

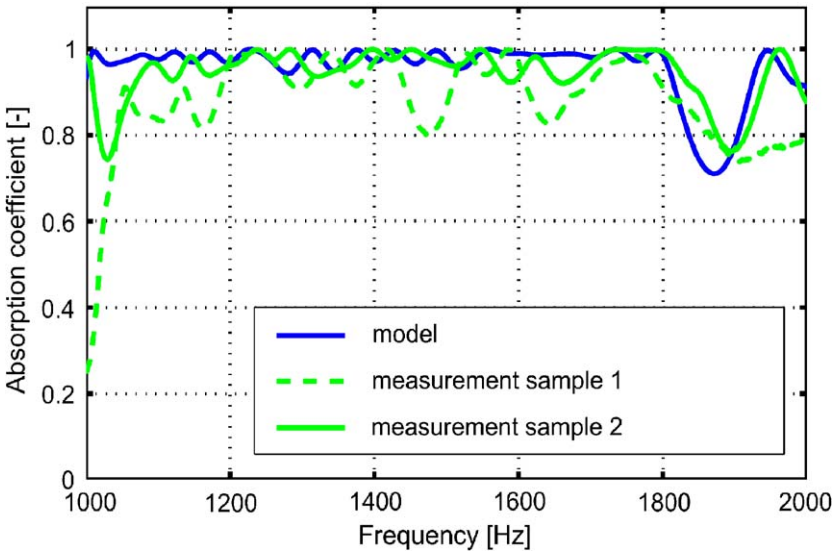

Fig. 28. Measured and calculated absorption coefficient.

certain conditions, the Microflown results are more accurate than those from conventional microphones.

[by R. Visser & H. Tijdeman, University of Twente, Netherlands]

9.4. Discontinuous Galerkin methods for aeroacoustics

The EU project MESSIAEN is focused on the convected propagation of the tonal noise produced by turbomachines. The concept is to solve the linearized Euler equations (LEE) with a quadrature-free discontinuous Galerkin method on unstructured grids. This method, which solves the acoustic field near the source, is coupled with a Ffowcs-Williams/Hawkings method to predict the far-field acoustic pressure. Acoustic liners can be accounted for so enabling the design of quieter engines,. While special emphasis is put on large nacelle problems, with Helmholtz numbers of up to 50 for three-dimensional geometries, the software will be validated for the convected propagation of tonal noise in non-isothermal flows encountered, for example, at the exhaust of helicopter engines. The project is coordinated by Free Field Technologies (Belgium) with partners Airbus, Rolls Royce, Turbomeca, Liebherr, Aermacchi, UCL, ISVR, TUE, Vibratec, ODS.

[by X. Gallez, P. Ploumhans, S. Caro, FFT, Belgium]

9.5. High order discontinuous Galerkin (DG) schemes

The numerical approximation of aeroacoustic wave propagation in complex domains is still a major challenge. Usually, the quality of the numerical results strongly depends on the regularity of the grid. Dumbser and Munz [22] showed that high-order discontinuous Galerkin (DG)-schemes behave very well even on non-regular unstructured grids and are able to produce the good accuracy in practical calculations. The finite-volume ADER (arbitrary order using derivatives)

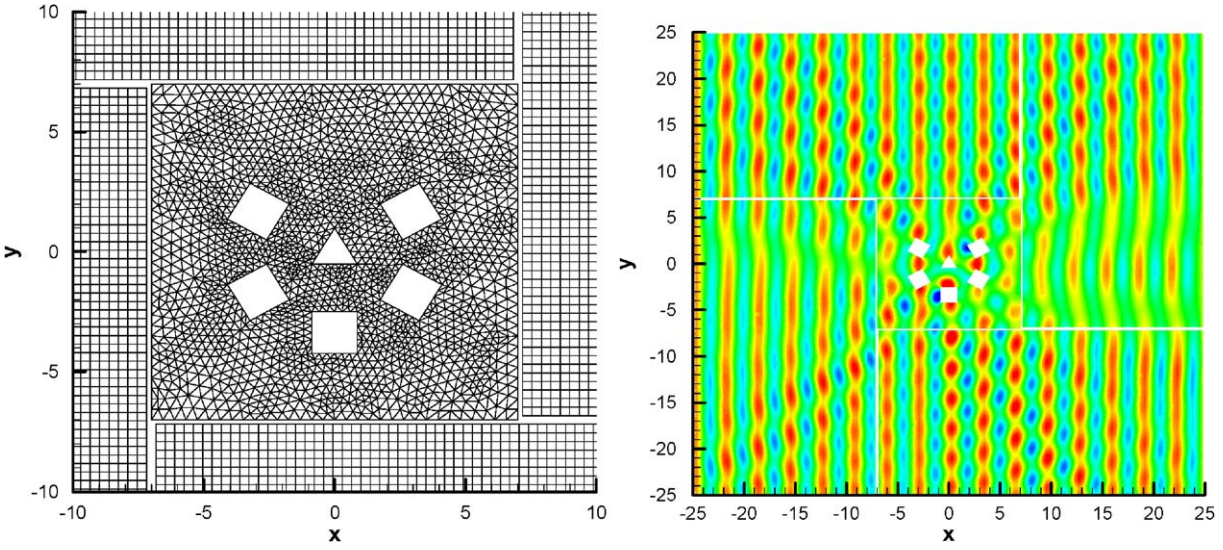

Fig. 29. Plane wave scattered at obstacles and the corresponding grid for this calculation with a scheme, sixth order accurate in space and time.

approach to the finite-element framework was extended further and the DG-schemes on unstructured grids combined with fast ADER finite-volume schemes on Cartesian grids away from the obstacles by Schwtzkopff et al. [23]. The results from this are shown in Fig. 29.

[by M. Dumbser, C.-D. Munz, Universität Stuttgart, Germany]

9.6. High-order curvilinear simulations of flows around non-Cartesian bodies

High-order schemes typically require large stencils, and are therefore generally implemented on structured grids. However, complex curved geometries are often impossible to mesh with a structured Cartesian grid without resorting to extrapolation techniques for the implementation of solid boundary conditions. The difficulty can be overcome by the use of curvilinear transformations combined with overset multiple grid techniques, often referred to as Chimera techniques [24]. As an illustration, Fig. 30 shows the diffraction of sound by two circular cylinders of different diameters.

[by O. Marsden, C. Bogey and C. Bailly, Ecole Centrale de Lyon, France]

10. Miscellaneous topics

10.1. Analysis of the aeroacoustics of the VEGA launcher to estimate the payload vibroacoustic environment

An investigation of the aeroacoustic environment created by the external aerodynamics around the VEGA launcher has been carried out by AVIO, CIRA (Italian Aerospace Research Centre),

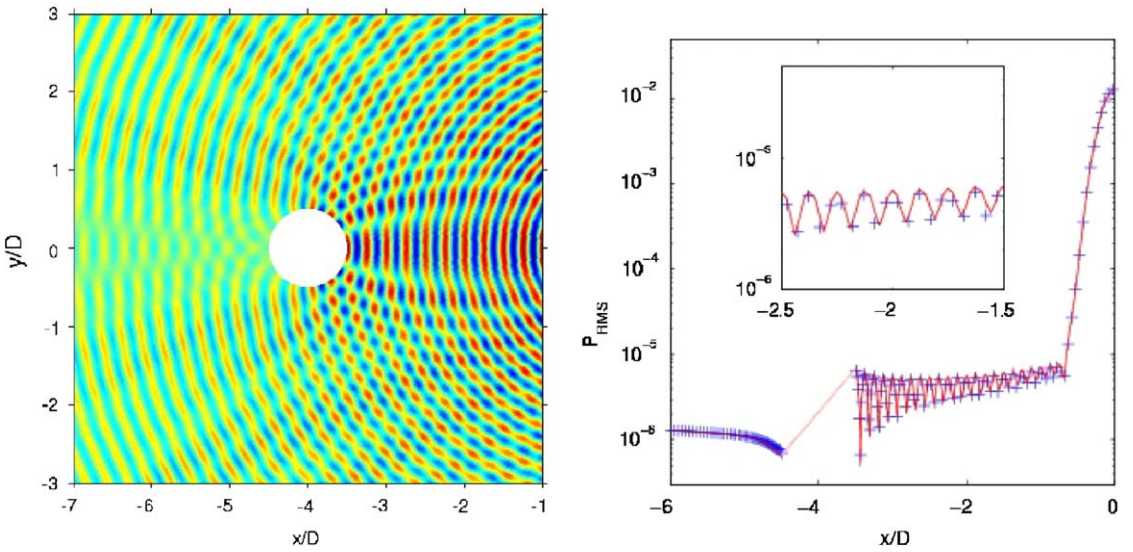

Fig. 30. Diffraction of sound by two cylinders. (Snapshot of the fluctuating pressure field and comparison of the RMS pressure around the larger cylinder along the x-axis with analytical solution).

and the Department of Mechanical and Industrial Engineering of the University "Roma Tre". The objective was to determine the pressure fluctuations perceived by the panel structures and to estimate the payload vibroacoustic environment. The pressure field was characterized and addressed through wind tunnel tests at transonic and supersonic flow conditions on a 1:30 scale model. The model was equipped with 32 *unsteady* pressure transducers placed on the model lee side generatrix in the symmetry plane; some of them were installed in clusters to form a network in order to estimate correlations functions, cross-spectra, coherence, and other information necessary to tune the aeroacoustic model for the turbulent boundary layer (TBL) excitation. Four accelerometers were placed at the foremost and rearmost possible locations along both the longitudinal and normal directions. The experimental data were analysed in order to obtain reliable predictions of the wall pressure fluctuations properties on the full-scale launcher in actual flow conditions. A theoretical model of the TBL noise was defined, which allowed for the exploitation of the experimental data to determine the full-scale pressure fluctuation properties of interest.

The full-scale extrapolation procedure was developed following three steps:

1. Evaluation of the integral boundary layer properties following a theoretical/numerical approach based on the integral formulation of the simplified governing equations for the case of an axi-symmetric compressible boundary layer in laminar and turbulent conditions.
2. Definition of a semi-empirical model of the fluctuating pressure field acting on the external surface of the scaled model and definition of the scaling method to be adopted for recovering full-scale predictions. This task was pursued on one side by selecting a suitable model among those already available in literature and on the other by creating ad hoc analytical models aimed at reproducing more accurately the spectral quantities.

3. Development of software aimed at processing the raw data from the pressure transducers to determine quantities of interest for the theoretical models.
   [by A. Nicolì, B. Imperatore (CIRA), G. Guj, R. Camussi (University ''Roma Tre''), A. Pizzicaroli (AVIO), Italy]

10.2. A test capability for studying cruise noise

The noise levels experienced by passengers within the aircraft cabin during cruise is a significant issue, especially for long range aircraft. During cruise, while jet mixing noise is relatively weak, the pressure ratio of the engine propulsion nozzles is supercritical and quite strong shock noise is generated. The bypass flow, and possibly the core flow, becomes supersonic under these conditions and shocks form in a regular pattern along the exhaust plume. The interaction of the shocks with the jet turbulence generates shock-associated noise, the presence of which is well known on military aircraft. To satisfy the cruise noise requirements of airlines and aircraft manufacturers, methods of reducing or alleviating the shock noise, which is broadband in character and of relatively high frequency, are being pursued. As little is known of shock noise specific to modern high-bypass ratio turbofan engines, an experimental research programme is being carried out at model-scale in the enhanced Noise Test Facility at QinetiQ, Farnborough. For this purpose, a special ''cruise'' tunnel has been designed, manufactured and commissioned. The tunnel is attached to the existing flight stream duct work and has been shown to simulate cruise Mach numbers of over 0.8 in a 1.05 m^2 working section. The working section, approximately 2 m long, is fitted with acoustic lining allowing the jet noise measurements. Details of the facility are shown in Fig. 31. The results from this work will be used to validate low cruise-noise devices and to develop and extend the near-field noise prediction work previously developed under the UK MOD Applied Research Programme on acoustic fatigue.

[by M. Harper-Bourne, QinetiQ Ltd, UK]

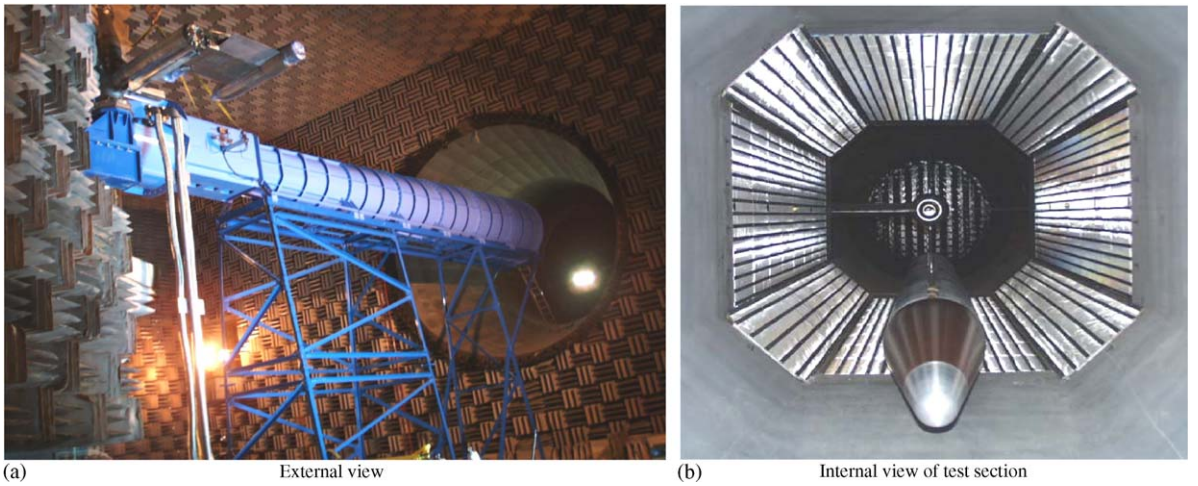

(a) External view (b) Internal view of test section

Fig. 31. NTF tunnel for cruise noise.

10.3. Sound engineering for aircraft (SEFA)

The SEFA project supported by the EC, 6th framework program involves 20 partners from 8 different countries. It involves a completely unique and innovative approach for exterior aircraft noise control by applying sound engineering practices, which have been used for a wide range of technical areas. SEFA is the first project using these practices to define optimum aircraft community noise shapes (target sounds). For this extensive psychometric testing is planned within an intercultural environment. In a second step, aircraft technology design criteria will be defined to meet these target sounds. This process involves innovative simulation tools: virtual aircraft and virtual resident. The aim of SEFA is to answer how the noise annoyance of aircraft can be reduced, not just by lowering noise levels, but also by improving the characteristics of aircraft noise signatures in the context of airport operations. In the current stage of SEFA the initialization phase has been concluded. Psychometric pre-tests have been undertaken, the first main psychometric test campaign is going to be started soon. In parallel the tool development for target sound design, virtual aircraft design as well as virtual resident design has started.

[by R. Drobietz, DaimlerChrysler R&T, Dornier GmbH, Germany]

References

[1] S. Lewy, Inverse method predicting spinning modes radiated by a ducted fan from free-field measurements, *Journal of the Acoustical Society of America* 117 (2) (2005).

[2] G. Rahier, J. Prieur, F. Vuillot, N. Lupoglazoff, A. Biancherin, Investigation of integral surface formulations for acoustic post-processing of unsteady aerodynamic jet simulations, *Aerospace Science and Technology* 8 (6) (2004) 453–467.

[3] F. Vuillot, G. Rahier, N. Lupoglazoff, J. Prieur, A. Biancherin, Comparative jet noise computations using a coupled CFD-acoustic solution, *Proceedings of the 11th International Congress on Sound and Vibration (ICSV11)*, 5–8 July 2004, Saint-Petersburg, Russia.

[4] M.J. Fisher, G.A. Preston, W.D. Bryce, A modelling of the noise for simple coaxial jets, part I: with unheated primary flow, *Journal of Sound and Vibration* 209 (3) (1998) 385–403.

[5] M.J. Fisher, G.A. Preston, C.J. Mead, A modelling of the noise for simple coaxial jets, part II: with heated primary flow, *Journal of Sound and Vibration* 209 (3) (1998) 405–417.

[6] C.L. Morfey, V.M. Szewczyk, B.J. Tester, New scaling laws for hot and cold jet mixing noise based on a geometric acoustic model, *Journal of Sound and Vibration* 61 (2) (1978) 255–292.

[7] N.C. Ovenden, W. Eversman, W., S.W. Rienstra, Cut-on cut-off transition in flow ducts: comparing multiple-scales and finite-element solutions, *10th AIAA/CEAS Aeroacoustics Conference*, Manchester, UK, May 2004, Paper AIAA-2004-2945.

[8] N.C. Ovenden, A uniformly valid multiple scales solution for cut-on cut-off transition of sound in flow ducts, *Journal of Sound and Vibration* 286 (2005) 403–416.

[9] R.M. Munt, Acoustic transmission properties of a jet pipe with subsonic jet flow: I. The cold jet reflection coefficient, *Journal of Sound and Vibration* 142 (1990) 413–436.

[10] M.S. Howe, The damping of sound by wall turbulent sheer layers, *Journal of the Acoustical Society of America* 98 (3) (1995) 1723–1730.

[11] E. Dokumaci, A note on transmission of sound in a wide pipe with mean flow and viscothermal attenuation, *Journal of Sound and Vibration* 208 (4) (1997) 653–655.

[12] W.P. Bi, V. Pagneux, D. Lafarge, Sound propagation in varying cross section ducts lined with nonuniform impedance, I: local rigid modes expansion, *AIAA/CEAS Aeroacoustics Conference*, 2005, AIAA Paper 2005-3066.

[13] S. Hein, T. Hohage, W. Koch, On resonances in open systems, *Journal of Fluid Mechanics* 506 (2004) 255–284.

[14] W. Koch, Acoustic resonances in rectangular open cavities, *AIAA/CEAS Aeroacoustics Conference*, 2004, AIAA Paper 2004-2843.
[15] S. Hein, W. Koch, J. Schöberl, Acoustic resonances in a 2D high lift configuration and 3D open cavity, *AIAA/CEAS Aeroacoustics Conference*, 2005, AIAA Paper 2005-2867.
[16] M. Pott-Pollenske, J. Alvarez-Gonzales, W. Dobrzynski, Effect of slat gap on farfield noise and correlation with local flow characteristics, *AIAA/CEAS Aeroacoustics Conference*, 2003, AIAA Paper 2003-3228.
[17] R. Ewert, W. Schröder, Acoustic perturbation equations based on flow decomposition via source filtering, *Journal of Comparative Physics* 188 (2003) 365–398.
[18] R. Ewert, W. Schröder, On the simulation of trailing edge noise with a hybrid LES/APE method, *Journal of Sound and Vibration* 270 (2004) 509–524.
[19] J. Yin, P. Spiegel, H. Buchholz, Towards noise abatement flight procedure design: DLR rotorcraft noise ground footprints model and its validation, *30th European Rotorcraft Forum*, 14–16 September 2004, Marseilles, France.
[20] J. Yin, S. Ahmed, Helicopter main-rotor/tail–rotor interaction, *Journal of the American Helicopter Society* 45 (4) (2000) 293–302.
[21] J.P. Battaner-Moro, New Automated Source Breakdown Algorithm for Jet Noise, *AIAA/CEAS Aeroacoustics Conference*, 2003, AIAA Paper 2003-3324.
[22] M. Dumbser, C.-D. Munz, Building blocks for arbitrary high order discontinuous Galerkin schemes, *Journal of Scientific Computing*, in press.
[23] T. Schwartzkopff, M. Dumbser, C.-D. Munz, CAA using domain decomposition and high order methods on structured and unstructured meshes, *AIAA/CEAS Aeroacoustics Conference*, 2004.
[24] O. Marsden, C. Bogey, C. Bailly, High-order curvilinear simulations of flows around non-Cartesian bodies, *AIAA/CEAS Aeroacoustics Conference*, 2004, AIAA Paper 2004-2813.